Progression of the late-stage divisome is unaffected by the depletion of the cytoplasmic FtsZ pool

Nadine Silber[1,2§], Christian Mayer[1,2§], Cruz L Matos de Opitz[1,2], Peter Sass[1,2*]

[1]Department of Microbial Bioactive Compounds, Interfaculty Institute of Microbiology and Infection Medicine, University of Tübingen, Auf der Morgenstelle 28, 72076 Tübingen, Germany

[2]Cluster of Excellence - Controlling Microbes to Fight Infections, University of Tübingen, Germany

[§] These authors contributed equally

[*]Correspondence should be addressed to Peter Sass (peter.sass@uni-tuebingen.de)

Running title: Progression of the late-stage divisome is unaffected by the FtsZ pool

Keywords: cytokinesis, cell division, FtsZ ring, FtsZ treadmilling, antibiotics, ADEP, ClpP, PC190723

Abstract

Cell division is a central and essential process in most bacteria, and also due to its complexity and highly coordinated nature, it has emerged as a promising new antibiotic target pathway in recent years. We have previously shown that ADEP antibiotics preferably induce the degradation of the major cell division protein FtsZ, thereby primarily leading to a depletion of the cytoplasmic FtsZ pool that is needed for treadmilling FtsZ rings. To further investigate the physiological consequences of ADEP treatment, we here studied the effect of ADEP on the different stages of the FtsZ ring in rod-shaped bacteria. Our data reveal the disintegration of early FtsZ rings during ADEP treatment in *Bacillus subtilis*, indicating an essential role of the cytoplasmic FtsZ pool and thus FtsZ ring dynamics during initiation and maturation of the divisome. However, progressed FtsZ rings finalized cytokinesis once the septal peptidoglycan synthase PBP2b, a late stage cell division protein, colocalized at the division site, thus implying that the concentration of the cytoplasmic FtsZ pool and FtsZ ring dynamics are less critical during the late stages of divisome assembly and progression.

53 **Introduction**

54 Cell division is a vital process in most bacteria and ensures the generation of progeny, usually by
55 yielding equal daughter cells. In rod-shaped bacteria, such as *Bacillus subtilis*, cell division occurs
56 at midcell, driven by FtsZ and orchestrated by a diverse set of proteins together constituting the
57 divisome[1,2]. As the pacemaker of cell division, FtsZ self-polymerizes into protofilaments, which are
58 characterized by additional lateral interactions resulting in higher order polymer assemblies[3], to
59 finally build the FtsZ ring at the future division site. Here, the FtsZ ring acts as the scaffold for other
60 divisome members. During polymerization, the T7 loop of one FtsZ subunit inserts into the GTP
61 binding site of the next subunit, thereby triggering hydrolysis of GTP to GDP and favoring the
62 disassembly of FtsZ protofilaments[4,5]. Hence, there is a constant and rapid exchange of FtsZ
63 subunits between the dynamic FtsZ ring and the cytoplasmic pool of FtsZ[6-8]. As the cell cycle
64 proceeds, the divisome constricts and synthesizes septal peptidoglycan to allow for septum
65 formation and eventually cytokinesis. Consequently, the process of divisome assembly and
66 progression can be separated into different steps, for example, with regard to the attachment of
67 the FtsZ ring to the membrane, the extent of FtsZ ring constriction, or the consecutive arrival of
68 early and late cell division proteins[7,9,10]. Over the last years, principally two mechanisms have been
69 discussed on how the force required for cytokinesis is generated, either by the chemical energy
70 of FtsZ-dependent GTP hydrolysis[11,12], or alternatively by peptidoglycan synthesis[11,13]. Recently,
71 FtsZ treadmilling, the GTP-dependent dynamic exchange of FtsZ from the cytoplasmic pool with
72 the FtsZ ring, has been reported to drive divisome progression and constriction in rod-shaped
73 bacteria[14,15]. In cocci such as *Staphylococcus aureus*, however, cell division mainly occurs in two
74 steps in this context, an initial step involving FtsZ treadmilling and a second step that increasingly
75 depends on peptidoglycan synthesis[16]. In this study, we set out to further investigate the role of
76 the cytoplasmic FtsZ pool and FtsZ ring dynamics on the distinct steps of septum formation in rod-
77 shaped bacteria.

78

Results and Discussion

To examine the effect of the abundance of FtsZ on divisome assembly and progression, we employed antibiotics of the ADEP class as tools to rapidly modulate the cytoplasmic pool of FtsZ in the model organism *B. subtilis*. ADEP deregulates the bacterial caseinolytic protease, activating its dormant core ClpP for the untimely degradation of FtsZ[17,18]. ADEP incubation thus leads to an impressive filamentation phenotype of *B. subtilis* at concentrations close to the minimal inhibitory concentration (MIC)[18,19]. Very recently, we showed that ADEP-ClpP preferably targets the N terminus of monomeric FtsZ, leading to unfolding and degradation of the FtsZ N-terminal domain[20]. Intriguingly, N-terminal degradation was prevented upon nucleotide binding to FtsZ, most probably due to a stabilization of the FtsZ protein fold. Hence, at ADEP concentrations resulting in a filamentation phenotype, ADEP primarily leads to a depletion of the cytoplasmic pool of nucleotide-free FtsZ in the bacterial cell[20], thus reducing the FtsZ concentration below the critical level needed for FtsZ ring formation[21,22] and continuously removing available FtsZ required for FtsZ ring dynamics (Fig. 1a). In line with this, a recent model on cell-size homeostasis in rod-shaped bacteria described a direct correlation of FtsZ expression and accumulation on septal constriction initiation[23]. Therefore, ADEP was considered instrumental to investigate the role of the cytoplasmic FtsZ pool and FtsZ ring dynamics during divisome formation and progression. To do so, we first tested the effect of ADEP on polymerized FtsZ (in the presence of GTP) (Fig. 1b). Once assembled into protofilaments, FtsZ substantially resisted the degradation by ADEP-ClpP. It may thus be hypothesized that, if divisome assembly and constriction fully depend on the cytoplasmic FtsZ pool and FtsZ ring dynamics, ADEP treatment should result in the disintegration of early as well as late stage divisomes, or at least, the progression of late stage divisomes should be halted. To test this hypothesis, we conducted time-lapse and super-resolution fluorescence microscopy experiments with ADEP-treated *B. subtilis* strain 2020 using filamentation concentrations of the antibiotic. This strain additionally expresses FtsZ fused to GFP from an ectopic locus. For microscopy, ADEP-treated bacteria were mounted and then further grown on

105 microscopy slides coated with ADEP-supplemented agarose (approximate division time of
106 bacteria on microscopy slides was 30-45 minutes). Of note, ADEP leads to a depletion of the FtsZ
107 pool within 15-20 minutes, i.e. the cellular concentration of FtsZ is reduced by more than half
108 within 5 minutes of ADEP treatment, whereas biomass increase and metabolism in general remain
109 unaltered[18,20]. Therefore, the elapsed time between the addition of ADEP to the cells and initial
110 image acquisition was set to 15-20 minutes, ensuring that image acquisition started under FtsZ-
111 depleted conditions. By monitoring FtsZ ring formation over time, we observed that ADEP inhibited
112 the initiation of FtsZ ring assembly, and early FtsZ rings that had just been formed disintegrated.
113 Here, the presence of early FtsZ rings at the beginning of the experiment and their soon
114 disintegration indicate that imaging started just before ADEP effects on FtsZ rings could visually
115 be observed. However, in contrast to early FtsZ rings, more progressed FtsZ rings constricted and
116 finished septum formation, apparently being less sensitive to ADEP treatment, finally yielding two
117 separated daughter cells (Fig. 2ab, Supplementary Fig. 1 and 2, Supplementary Movies 1-3).
118 Following up on this, we investigated whether the arrival of the late stage cell division protein
119 PBP2b[9], a septal peptidoglycan synthase, would coincide with a successful constriction of
120 progressed FtsZ rings during ADEP-treatment. By using *B. subtilis* strain CM03, which allows for
121 the concomitant expression of mCherry-FtsZ and GFP-PBP2b, we observed that early FtsZ rings
122 disintegrated prior to the arrival of PBP2b. On the contrary, the divisome consistently finalized cell
123 division after PBP2b had substantially arrived at the septum area (Fig. 3ab, Supplementary Fig. 3,
124 Supplementary Movie 4). It may therefore be hypothesized that the arrival or activity of late stage
125 cell division proteins, such as peptidoglycan synthases, may substantially support or even trigger
126 divisome progression in rod-shaped bacteria similar as previously suggested for coccoid bacteria,
127 such as *S. aureus*[16].
128 At the same time, Whitley and colleagues published a preprint reporting a related observation
129 regarding the role of FtsZ treadmilling during cell division, however, using the antibiotic PC190723.
130 In contrast to ADEP, PC190723 stabilizes FtsZ bundles and halts FtsZ dynamics instead of

131 depleting FtsZ by fast degradation as occurs in ADEP-treated cells. In line with our observations,
132 FtsZ treadmilling had a dispensable function in accelerating septal constriction rate in their study,
133 while it was critical for assembling and initiating the bacterial divisome[24,25].
134 In conclusion, our data imply distinct stages during FtsZ ring initiation, maturation and constriction
135 in rod-shaped bacteria with regard to the role of the cytoplasmic FtsZ pool as well as the sensitivity
136 to ADEP antibiotics. Clearly, during ADEP treatment it is distinguished between early and more
137 progressed divisomes, thereby adding another level of complexity to the elaborate mechanism of
138 ADEP action. Also, our data support a two-step model of cell division in *B. subtilis* (Fig. 4), in which
139 the late-stage divisome is substantially less sensitive to a depletion of the cytoplasmic FtsZ pool,
140 and thus less dependent on FtsZ ring dynamics, in contrast to initial assembly and early stage
141 FtsZ rings.
142
143 **Methods**
144 **Protein purification**
145 FtsZ and ClpP proteins were derived from *B. subtilis* 168 (*trpC2*; wild-type strain; NC_000964.3)
146 and were expressed as C-terminally His_6-tagged proteins in *E. coli* BL21(DE3) harboring the
147 respective expression plasmid[18,20]. Expression cultures were grown in lysogeny broth (LB)
148 containing ampicillin (100 µg/ml) to an optical density at 600 nm (OD_{600}) of 0.6. Then protein
149 expression was induced by the addition of isopropyl-β-D-thiogalactopyranoside (IPTG) to a final
150 concentration of 1 mM. Expression cultures were harvested after 4 hours followed by standard
151 protein purification steps under native conditions using Ni-NTA affinity chromatography. Quantity
152 and quality of the purified proteins were verified by Bradford assay (using bovine serum albumin
153 as control), Nanodrop spectrophotometry (Nanodrop Technologies) and SDS-PAGE. We have
154 shown previously that purification-tags have no effect on FtsZ degradation or enzyme activity of
155 both proteins[20].
156

157 ***In vitro* FtsZ polymerization and degradation assays**

158 For GTP-dependent polymerization of FtsZ *in vitro*[26,27], purified *B. subtilis* 168 FtsZ (25 µM) was
159 preincubated in polymerization buffer (50 mM MES/NaOH, pH 6.5, 50 mM KCl, 10 mM $MgCl_2$) for
160 10 min on ice. After initial incubation for 4 min at 37 °C allowing baseline correction, GTP was
161 added to the respective reaction mixture to a final concentration of 1 mM. Then, reaction mixtures
162 were transferred into a photometer cuvette for monitoring light transmission at 400 nm and 37 °C
163 over time. For *in vitro* degradation of polymerized FtsZ, 12 µM ADEP2[17,28] (or equal volume of
164 DMSO as a control) and 1.5 µM purified ClpP protein (monomer concentration) were added to the
165 polymerization reaction after 16 min, as indicated, and light transmission was further monitored
166 for 34 min. As an independent control, FtsZ (4 µM) was incubated with 1 mM GTP in activity buffer
167 (50 mM Tris/HCl pH 8, 25 mM $MgCl_2$, 100 mM KCl, 2 mM DTT) at 37 °C for 30 min. Then 1.5 µM
168 ClpP (monomer concentration) and 3.75 µM ADEP (or equal volume of DMSO as a control) were
169 added to the reaction mixtures that were further incubated at 37 °C. Samples were taken after
170 120 min and were analyzed via SDS-PAGE using standard techniques[18,20].

171

172 **Cloning strategy**

173 For colocalization studies of FtsZ with PBP2b (mCherry-FtsZ/GFP-PBP2b), strain *B. subtilis* CM03
174 was constructed as follows. Plasmid pHJCM03 was generated using the coding sequence of *pbpB*
175 that was amplified from chromosomal DNA of *B. subtilis* 168 (*trpC2*; wild-type strain;
176 NC_000964.3) *via* PCR using the following primers: oCM07
177 5'-GGAAGCGGCTCAGGCTCCCGGATCCACATTCAAATGCCAAAAAAGAATAAATTTATG-3',
178 oCM08 5'-CGCGGCCGCTCTAGAACTAGAATTCTTAATCAGGATTTTTAAACTTAACCTTG-3'.
179 The amplicon was then ligated into the linearized plasmid pHJCM01[19] by a Gibson isothermal
180 reaction. The resulting plasmid was transformed into *B. subtilis* CM01 (*trpC2 cat aprE::Pspac-*
181 *mcherry-ftsZ*)[19] to give strain CM03 (*trpC2 cat aprE::Pspac-mcherry-ftsZ; spc amyE::Pxyl-msfgfp-*
182 *pbpB*).

183 **Super-resolution and time-lapse fluorescence microscopy**

184 Cells of *B. subtilis* 2020 (*trpC2 spc amyE::Pxyl-gfp-ftsZ*)[29] or *B. subtilis* CM03 (*trpC2 cat*
185 *aprE::Pspac-mcherry-ftsZ; spc amyE::Pxyl-msfgfp-pbpB*) were grown at 37 °C to early-
186 exponential phase (OD_{600} of 0.1). For the expression of GFP and mCherry fusion proteins, *Pxyl*
187 and *Pspac* promoters were induced using 0.1-0.2% xylose and 0.1 mM IPTG, respectively. Then,
188 cells were pre-incubated in lysogeny broth (LB) supplemented with 0.125-0.25 µg/ml ADEP2 for
189 10 minutes or DMSO as a control. Bacteria were transferred onto microscopy slides using gene
190 frames (Life Technologies) and a thin film of 1.5% agarose in 25% LB containing 0.125-0.25 µg/ml
191 ADEP2 as well as according concentrations of the inducer compounds xylose and/or IPTG.
192 Doubling times of bacteria on microscopy slides were in the range of 30-45 minutes. Phase
193 contrast and fluorescence images were taken at distinct time points as indicated. Elapsed time
194 between sampling and image acquisition was approximately 5-10 minutes. Of note, the ADEP2
195 concentration used here results in filamentation of *B. subtilis*, resembling a phenotype that is due
196 to fast FtsZ degradation, i.e. the cellular amount of FtsZ is reduced by more than half within 5
197 minutes once ADEP-ClpP is fully engaged, whereas biomass increase and metabolism in general
198 remain unaltered[18]. Since the addition of ADEP leads to an overall depletion of the FtsZ pool within
199 15-20 minutes[18,20], image acquisition was started at the assumed onset of detectable FtsZ pool
200 reduction (correlating to approximately half the bacterial doubling time on microscopy slides),
201 which is further indicated by the presence of early FtsZ rings at the start of imaging as well as their
202 soon disintegration. For image analyses, we deliberately monitored bacterial cells or small cell
203 clusters (i.e. immediate daughter cells) that showed both early as well as late FtsZ rings, thereby
204 ensuring similar conditions of ADEP action on the distinct stages of the FtsZ ring and the divisome
205 in the analyzed bacterial cells. Super-resolution images were recorded using a Zeiss Axio
206 Observer Z1 LSM800 equipped with an Airyscan detector and a C Plan-Apo 63x/1.4 Oil DIC
207 objective (Zeiss, Germany). Images were processed using the ZEN2.3 image analysis software
208 package (Zeiss). Time-lapse micrographs were obtained using a Nikon Eclipse Ti automated

209 microscope equipped with a Perfect Focus system (Nikon Instruments Europe BV, Netherlands),
210 an Orca Flash 4.0 camera (Hamamatsu, Photonics, Japan) and CFI Plan-Apo DM 100x/1.45 Oil
211 Ph3 objective (Nikon). Image acquisition and analysis were performed via the NIS elements AR
212 software package (Nikon).
213

214 **Statistics and Reproducibility**

215 Microscopy and *in vitro* FtsZ degradation results were each obtained from at least three
216 independent experiments and biological samples. The results describing the effect of *in vitro*
217 degradation of FtsZ polymers on light transmission (Fig. 1b) are based on two independent
218 experiments. For experiments using samples of small sizes (Fig. 1b, N=2) mean values were
219 calculated and depicted, indicating individual data points via the bottom and top values of the
220 respective indicator bars. For the evaluation of the fate of divisomes (localization of FtsZ and
221 PBP2b) upon ADEP treatment, large numbers of divisomes (>950) from a total of twelve
222 independent biological samples were examined. Total values and percentages are described
223 (Supplementary Fig. 5 and 6).
224

225 **Data availability**

226 Additional datasets generated and/or analyzed during the current study are available from the
227 corresponding author on reasonable request.
228

229 **Acknowledgments**

230 We thank Heike Brötz-Oesterhelt for providing ADEP2, as well as Leendert Hamoen, Jeff
231 Errington and Kürşad Turgay for the kind gift of strains and plasmids. We also thank Anne
232 Berscheid for critically reading and discussing the manuscript.
233 The authors appreciate funding by the Deutsche Forschungsgemeinschaft (DFG, German
234 Research Foundation): Project-ID 398967434 (TRR 261-A02), the German Center for Infection

Research (DZIF; TTU 09.815), as well as support by infrastructural funding from the Cluster of Excellence EXC 2124 Controlling Microbes to Fight Infections.

Author contributions

N Silber, C Mayer, CL Matos de Opitz and P Sass performed and designed experiments, analyzed data and prepared figures. P Sass conceived and supervised the study, wrote the manuscript and raised funding. All authors discussed data and edited the manuscript.

Competing interests

The authors declare no competing interests.

References

1 den Blaauwen, T., Hamoen, L. W. & Levin, P. A. The divisome at 25: the road ahead. *Curr. Opin. Microbiol.* **36**, 85-94, (2017).
2 Silber, N., Matos, C., Mayer, C. & Sass, P. Cell division protein FtsZ: from structure and mechanism to antibiotic target. *Fut. Microbiol.* **15**, 801-831, (2020).
3 Sundararajan, K. & Goley, E. D. The intrinsically disordered C-terminal linker of FtsZ regulates protofilament dynamics and superstructure *in vitro*. *J. Biol. Chem.* **292**, 20509-20527, (2017).
4 Scheffers, D. J., de Wit, J. G., den Blaauwen, T. & Driessen, A. J. GTP hydrolysis of cell division protein FtsZ: evidence that the active site is formed by the association of monomers. *Biochemistry* **41**, 521-529, (2002).
5 Scheffers, D. J. & Driessen, A. J. Immediate GTP hydrolysis upon FtsZ polymerization. *Mol. Microbiol.* **43**, 1517-1521, (2002).
6 Addinall, S. G., Cao, C. & Lutkenhaus, J. Temperature shift experiments with an *ftsZ*84(Ts) strain reveal rapid dynamics of FtsZ localization and indicate that the Z ring is required throughout septation and cannot reoccupy division sites once constriction has initiated. *J. Bacteriol.* **179**, 4277-4284, (1997).
7 Erickson, H. P., Anderson, D. E. & Osawa, M. FtsZ in bacterial cytokinesis: cytoskeleton and force generator all in one. *Microbiol. Mol. Biol. Rev.* **74**, 504-528, (2010).
8 Sun, Q. & Margolin, W. FtsZ dynamics during the division cycle of live *Escherichia coli* cells. *J. Bacteriol.* **180**, 2050-2056, (1998).
9 Gamba, P., Veening, J. W., Saunders, N. J., Hamoen, L. W. & Daniel, R. A. Two-step assembly dynamics of the *Bacillus subtilis* divisome. *J. Bacteriol.* **191**, 4186-4194, (2009).
10 Walker, B. E., Männik, J. & Männik, J. Transient membrane-linked FtsZ assemblies precede Z-Ring formation in *Escherichia coli*. *Curr. Biol.* **30**, 499-508.e6, (2020).
11 Coltharp, C. & Xiao, J. Beyond force generation: Why is a dynamic ring of FtsZ polymers essential for bacterial cytokinesis? *Bioessays.* **39**, 1-11, (2017).
12 Li, Z., Trimble, M. J., Brun, Y. V. & Jensen, G. J. The structure of FtsZ filaments *in vivo* suggests a force-generating role in cell division. *Embo J.* **26**, 4694-4708, (2007).

13 Coltharp, C., Buss, J., Plumer, T. M. & Xiao, J. Defining the rate-limiting processes of bacterial cytokinesis. *Proc. Natl. Acad. Sci. USA* **113**, E1044-1053, (2016).
14 Bisson-Filho, A. W. *et al.* Treadmilling by FtsZ filaments drives peptidoglycan synthesis and bacterial cell division. *Science* **355**, 739-743, (2017).
15 Yang, X., Lyu, Z., Miguel, A., McQuillen, R., Huang, K. C. & Xiao, J. GTPase activity-coupled treadmilling of the bacterial tubulin FtsZ organizes septal cell wall synthesis. *Science* **355**, 744-747, (2017).
16 Monteiro, J. M. *et al.* Peptidoglycan synthesis drives an FtsZ-treadmilling-independent step of cytokinesis. *Nature* **554**, 528-532, (2018).
17 Brötz-Oesterhelt, H. *et al.* Dysregulation of bacterial proteolytic machinery by a new class of antibiotics. *Nat. Med.* **11**, 1082-1087, (2005).
18 Sass, P., Josten, M., Famulla, K., Schiffer, G., Sahl, H. G., Hamoen, L. & Brötz-Oesterhelt, H. Antibiotic acyldepsipeptides activate ClpP peptidase to degrade the cell division protein FtsZ. *Proc. Natl. Acad. Sci. USA* **108**, 17474-17479, (2011).
19 Mayer, C., Sass, P. & Brötz-Oesterhelt, H. Consequences of dosing and timing on the antibacterial effects of ADEP antibiotics. *Int. J. Med. Microbiol.* **309**, 151329, (2019).
20 Silber, N., Pan, S., Schäkermann, S., Mayer, C., Brötz-Oesterhelt, H. & Sass, P. Cell division protein FtsZ is unfolded for N-terminal degradation by antibiotic-activated ClpP. *mBio* **11**, e01006-01020, (2020).
21 Huecas, S., Llorca, O., Boskovic, J., Martin-Benito, J., Valpuesta, J. M. & Andreu, J. M. Energetics and geometry of FtsZ polymers: nucleated self-assembly of single protofilaments. *Biophys. J.* **94**, 1796-1806, (2008).
22 Mukherjee, A. & Lutkenhaus, J. Dynamic assembly of FtsZ regulated by GTP hydrolysis. *EMBO J.* **17**, 462-469, (1998).
23 Si, F., Le Treut, G., Sauls, J. T., Vadia, S., Levin, P. A. & Jun, S. Mechanistic Origin of Cell-Size Control and Homeostasis in Bacteria. *Curr. Biol.* **29**, 1760-1770.e1767, (2019).
24 Whitley, K. D. *et al.* FtsZ treadmilling is essential for Z-ring condensation and septal constriction initiation in bacterial cell division. *bioRxiv* 2020.07.01.182006. Preprint at *https://doi.org/10.1101/2020.07.01.182006*, (2020).
25 Silber, N., Mayer, C., Matos, C. & Sass, P. Progression of the late-stage divisome is unaffected by the depletion of the cytoplasmic FtsZ pool. *bioRxiv* 2020.06.30.180018. Preprint at *https://doi.org/10.1101/2020.06.30.180018*, (2020).
26 Krol, E. & Scheffers, D. J. FtsZ polymerization assays: simple protocols and considerations. *J. Vis. Exp.*, e50844, (2013).
27 Scheffers, D. J., den Blaauwen, T. & Driessen, A. J. Non-hydrolysable GTP-gamma-S stabilizes the FtsZ polymer in a GDP-bound state. *Mol. Microbiol.* **35**, 1211-1219, (2000).
28 Hinzen, B. *et al.* Medicinal chemistry optimization of acyldepsipeptides of the enopeptin class antibiotics. *ChemMedChem.* **1**, 689-693, (2006).
29 Stokes, N. R. *et al.* Novel inhibitors of bacterial cytokinesis identified by a cell-based antibiotic screening assay. *J. Biol. Chem.* **280**, 39709-39715, (2005).

321 **Figures legends**

322 **Fig. 1: ADEP antibiotics lead to a reduction of the cytoplasmic FtsZ pool.**

323 **a**, Schematic of ADEP-dependent degradation of FtsZ. ADEP (orange) activates bacterial ClpP
324 peptidase (blue) for untimely protein degradation, and nucleotide-free, monomeric FtsZ (dark
325 green) represents a preferred protein substrate for ADEP-ClpP[18,20]. As a consequence, the
326 cytoplasmic FtsZ pool is depleted (indicated by the shift from dark to light green), whereas GTP-
327 bound FtsZ (GTP in yellow) is stabilized against proteolytic attack at antibiotic concentrations close
328 to the MIC. FtsZ ring assembly relies on the dynamic exchange of FtsZ subunits between the FtsZ
329 ring and the cytoplasmic FtsZ pool (indicated by dark blue arrow). In the presence of ADEP, the
330 depletion of the FtsZ pool ultimately results in an inhibition of FtsZ ring formation and cell division,
331 finally leading to bacterial cell death. However, it remained unresolved, whether only early or also
332 later stages of the FtsZ-ring/divisome are affected by ADEP treatment.

333 **b**, *In vitro* FtsZ polymerization and FtsZ degradation by ADEP-activated ClpP. Light transmission
334 analyses of GTP-dependent FtsZ polymerization *in vitro* followed by incubation with a ClpP
335 reaction mixture in the absence or presence of ADEP and/or GTP (-GTP/-ADEP, in grey;
336 +GTP/-ADEP, in blue; +GTP/+ADEP, in orange). Here, polymerized FtsZ is not affected by
337 incubation with ADEP-ClpP. The graphs show mean values of two independent experiments,
338 bottom and top values of indicator bars show the individual data points of each respective
339 replicate. Source data underlying the graphs is presented in Supplementary Table 1. As an
340 independent control, we determined FtsZ protein amounts of samples that were incubated with or
341 without GTP for 120 min in the absence or presence of ADEP. DMSO was used as an untreated
342 control in all assays. Representative SDS-PAGE images of triplicates are depicted. Source data
343 of the full, uncropped gel image is presented in Supplementary Fig. 4.

344

345

346

347 **Fig. 2: Depletion of the FtsZ pool differently affects distinct stages of the FtsZ ring.**

348 **a,** Time-lapse fluorescence microscopy of exponentially growing *B. subtilis* 2020 cells treated with
349 0.25 µg/ml ADEP2. Overlaid fluorescence and phase contrast images show the localization of
350 GFP-tagged FtsZ (in green) and the progression of FtsZ rings over time. The micrographs indicate
351 that early FtsZ rings (open triangles) disintegrate during ADEP treatment while more progressed
352 FtsZ rings (closed triangles) constrict and finish septum formation to yield two separated daughter
353 cells. Numbers indicate previously finished septa. For clarity, numbers remain positioned to the
354 corresponding cell pole of the daughter cell on the right. A phase contrast image of bacterial cells
355 after 65 min is included at the end of the series to prove failure or success of septum formation.
356 Overlay (0-35 min) or single channel (65 min) images are provided. Scale bar, 5 µm. Images are
357 representative of at least three biological replicate cultures of *B. subtilis* 2020 with >600 FtsZ rings
358 analyzed over time. A time-lapse video is provided by Supplementary Movie 1.

359 **b**, Super-resolution fluorescence microscopy of different stages of FtsZ ring formation in *B. subtilis*
360 2020. While all of the early stage FtsZ rings disintegrate upon ADEP treatment (100%, N=323),
361 all late stage FtsZ rings further constrict and finalize septum formation (100%, N=140).
362 Intermediate stage FtsZ rings, which were in transition from early to late stages, show a
363 heterogeneous behavior with 71% of FtsZ rings abrogating division and 29% further constricting
364 and finalizing septum formation (N=178). Of note, we deliberately analyzed immediate daughter
365 cells comprising both early and further progressed FtsZ rings, of which all late stage FtsZ rings
366 finalized division while all early FtsZ rings did not, thus making it unlikely that the cells with late
367 stage FtsZ rings may by chance happened to have considerably higher FtsZ levels compared to
368 cells with early FtsZ rings. This is further supported by the fact that ADEP leads to a rapid depletion
369 of the FtsZ pool within 15-20 minutes, where potential minor differences of the FtsZ level may be
370 negligible in relation to the doubling time of the bacteria of approximately 30-45 minutes on
371 microscopy slides. Images are representative of at least three biological replicate cultures. Source
372 data underlying the graphs is presented in Supplementary Fig. 5.

373 **Fig. 3: The late-stage divisome progresses independent of the depletion of the FtsZ pool.**
374 **a**, Time-lapse fluorescence microscopy of exponentially growing *B. subtilis* CM03 cells treated
375 with 0.125 µg/ml ADEP2. Overlaid fluorescence and phase contrast images show the localization
376 of mCherry-FtsZ or GFP-PBP2b, as indicated, during ADEP treatment over time. The micrographs
377 show that the divisome consistently succeeds to finalize cell division (closed triangles) in the
378 presence of ADEP in situations when GFP-PBP2b is substantially detected at the septum area. In
379 contrast, early stage FtsZ rings, prior to the visible arrival of GFP-PBP2b at the septum,
380 disintegrate during ADEP treatment (open triangles). For clarity, a phase contrast image of
381 bacterial cells after 99 min is included at the end of the series to prove failure or success of septum
382 formation. Scale bar, 5 µm. Images are representative of at least three biological replicate cultures
383 of *B. subtilis* CM03 with >300 septa/FtsZ rings monitored over time. A time-lapse video is provided
384 by Supplementary Movie 4.
385 **b,** Quantification analysis assessing divisome progression and success of cell division in cells with
386 or without clear foci of PBP2b. In the absence of a substantial signal of GFP-PBP2b at the
387 divisome, early stage FtsZ rings disintegrate and cells fail to divide upon ADEP treatment (100%,
388 N=113), however, after substantial localization of GFP-PBP2b, the divisome progresses and cells
389 finalize septum formation and division (100%, N=174). In the transition phase of initial GFP-PBP2b
390 localization, cells show a heterogeneous behavior with 18.5% of the divisomes abrogating division
391 and 81.5% further constricting and finalizing division (N=27). Bottom panels show representative
392 fluorescence microscopy images of the different stages corresponding to the graphs in the upper
393 panel. Images are representative of at least three biological replicate cultures of *B. subtilis* CM03.
394 Source data underlying the graphs is presented in Supplementary Fig. 6.
395
396
397
398

399 **Fig. 4: Two-step model of FtsZ ring assembly and progression.**

400 At antibiotic concentrations close to the MIC, ADEP treatment essentially depletes the cytoplasmic
401 pool of FtsZ[20], thereby continuously removing available FtsZ that is needed for FtsZ ring formation
402 and dynamics[14]. Our data reveal that ADEP treatment leads to the disintegration of early FtsZ
403 rings (framed green) in *B. subtilis*, while more progressed FtsZ rings (framed red) resist
404 degradation and finish septum formation as well as daughter cell separation, suggesting distinct
405 stages during FtsZ ring initiation and progression. Therefore, our results support a two-step model
406 of FtsZ ring and divisome progression in *B. subtilis*. In the initial stage, FtsZ ring formation
407 essentially relies on the cytoplasmic FtsZ pool and FtsZ ring dynamics, indicated by the
408 disintegration of early FtsZ rings upon ADEP-dependent depletion of the cytoplasmic FtsZ pool.
409 In the later stage, the more progressed divisome is considerably less sensitive to a depletion of
410 the cytoplasmic FtsZ pool, implying that other triggers take over to drive divisome progression, for
411 example, peptidoglycan synthases that arrive at the divisome during the later stages of cell
412 division.

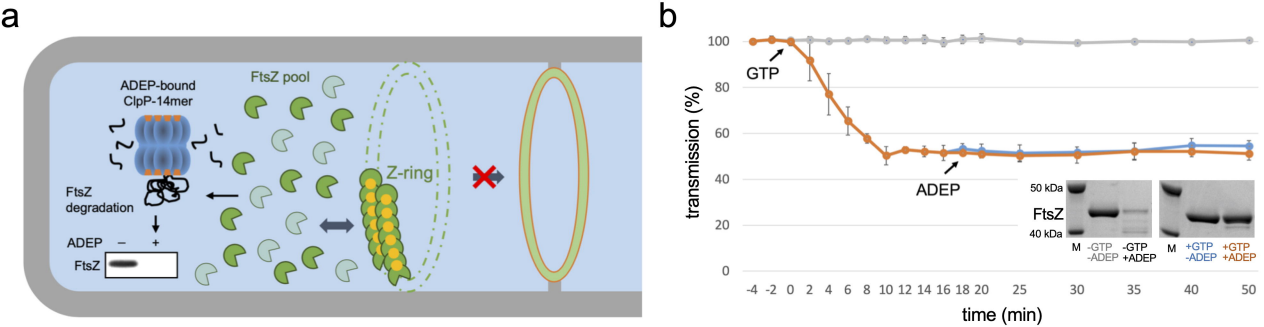
a
ADEP-bound
ClpP-14mer
FtsZ pool
Z-ring
FtsZ
degradation
ADEP
–
+
FtsZ
b
transmission (%)
100
80
60
40
20
0
GTP
ADEP
-4 -2 0 2 4 6 8 10 12 14 16 18 20 25 30 35 40 50
time (min)
50 kDa
FtsZ
40 kDa
M -GTP -GTP
-ADEP +ADEP
M +GTP +GTP
-ADEP +ADEP

a

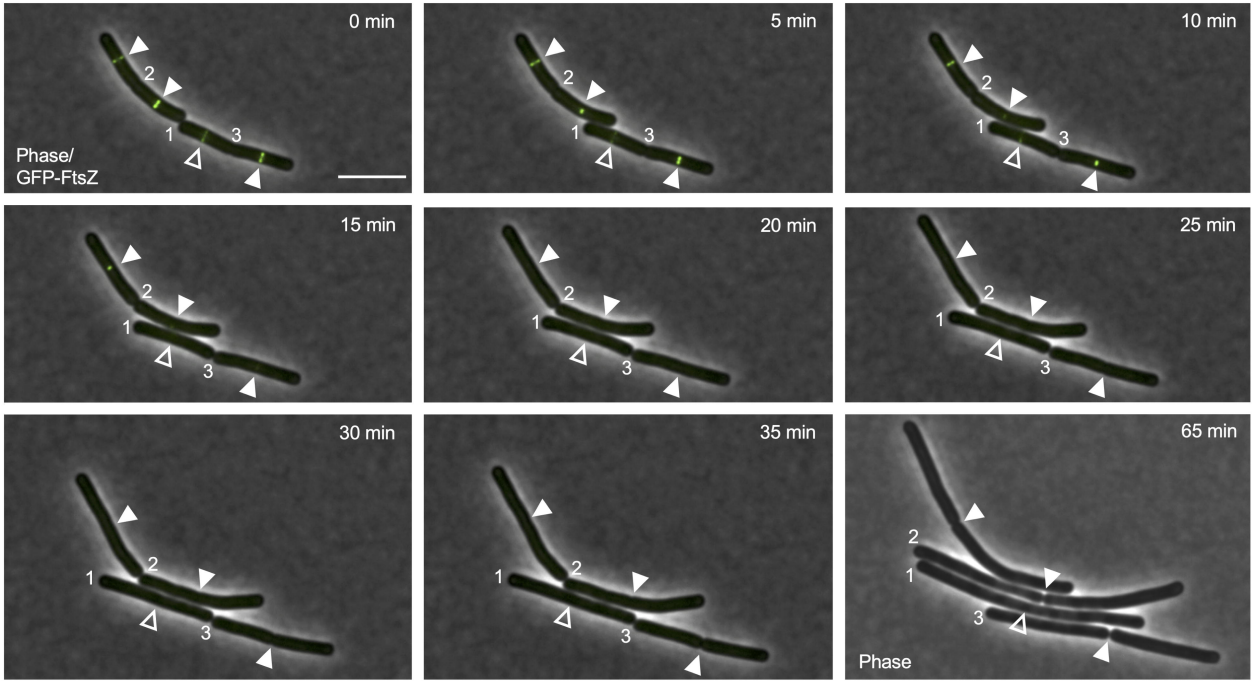
0 min
5 min
10 min
15 min
20 min
25 min
30 min
35 min
65 min
Phase/
GFP-FtsZ
Phase
1
2
3

b

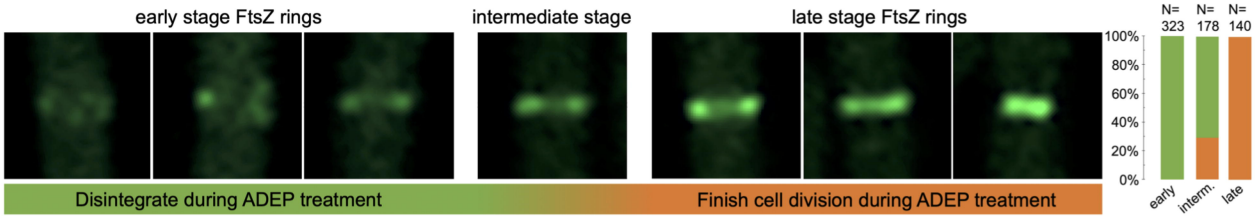
early stage FtsZ rings
intermediate stage
late stage FtsZ rings
Disintegrate during ADEP treatment
Finish cell division during ADEP treatment
N= 323
N= 178
N= 140
100%
80%
60%
40%
20%
0%
early
interm.
late

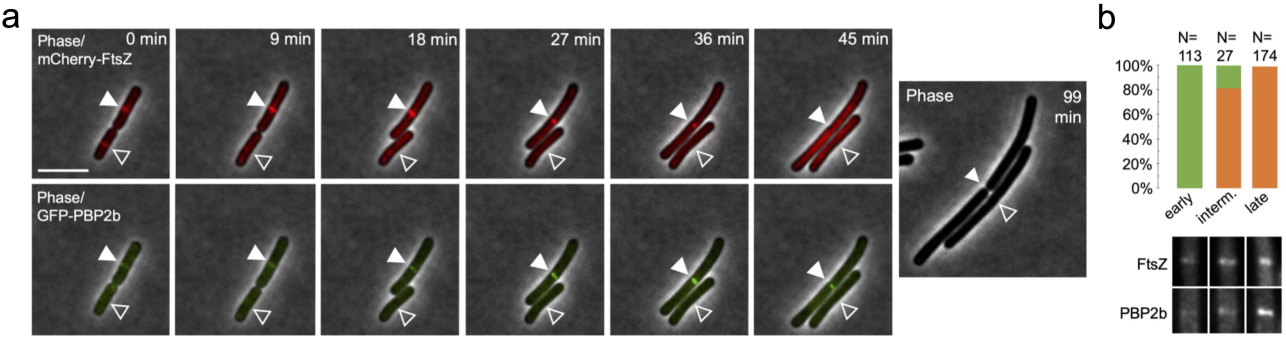
a
Phase/
mCherry-FtsZ
0 min
9 min
18 min
27 min
36 min
45 min
Phase/
GFP-PBP2b
Phase
99
min
b
N=
113
N=
27
N=
174
100%
80%
60%
40%
20%
0%
early
interm.
late
FtsZ
PBP2b

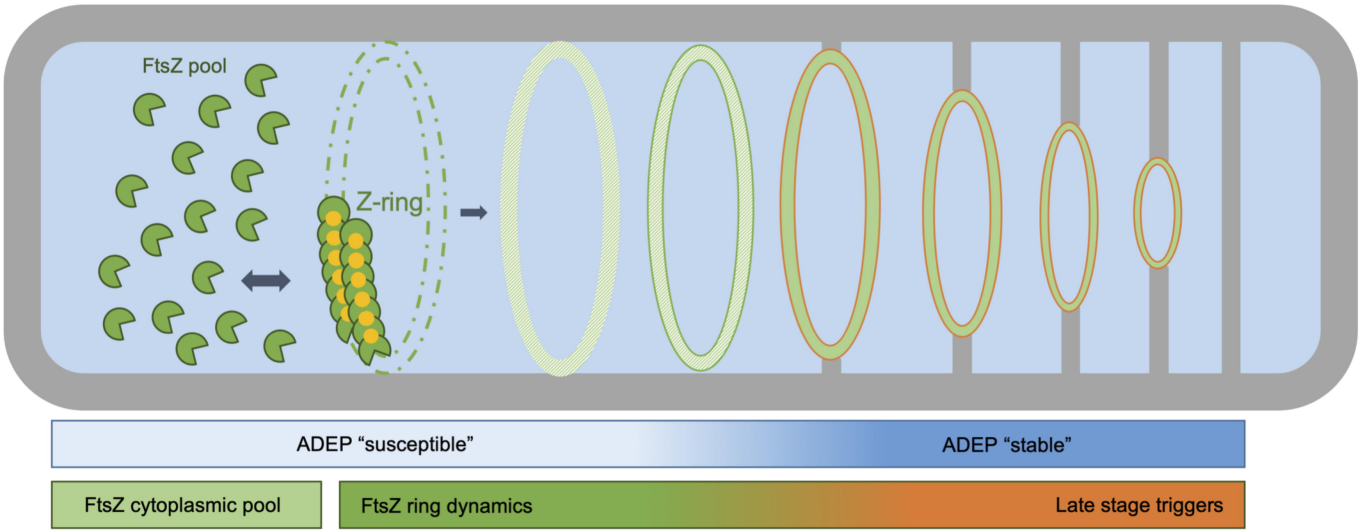
FtsZ pool
Z-ring
ADEP "susceptible"
ADEP "stable"
FtsZ cytoplasmic pool
FtsZ ring dynamics
Late stage triggers